The Angle between the Anticodon and Aminoacyl Acceptor Stems of Yeast tRNA^{Phe} Is Strongly Modulated by Magnesium Ions†

Marisa W. Friederich and Paul J. Hagerman*

Department of Biochemistry, Biophysics, and Genetics, University of Colorado Health Sciences Center, Denver, Colorado 80262

Received January 13, 1997; Revised Manuscript Received March 12, 1997⊗

ABSTRACT: Many tRNAs undergo tertiary folding transitions at temperatures well below the main thermally induced (hyperchromic) transition. Such transitions are essentially isochromic and isoenthalpic and display an absolute requirement for divalent cations; however, the nature of the structural transition is not known for any tRNA. Using a combination of transient electric birefringence (TEB) and gel electrophoretic measurements, we have characterized the influence of magnesium ions on the apparent angle between the anticodon and acceptor stems of a yeast tRNA^{Phe} construct. TEB is a particularly sensitive method for quantifying the bends introduced in RNA by various nonhelix elements. In the current instance, the tRNA construct comprises an unmodified tRNA^{Phe} molecule in which the anticodon and acceptor stems have been extended by ∼70 bp to more effectively "report" the interstem angles. Upon the addition of sub-millimolar concentrations of magnesium ions, the tRNA core undergoes a substantial rearrangement in tertiary structure, passing from an open form with an *apparent* interstem angle of ∼150° to a conformation with an interstem angle of ∼70° (200 μM Mg^{2+}). Further addition of magnesium ions results in a minor adjustment of the apparent interstem angle to ∼80−90°, in line with earlier results. Finally, the magnesium-induced structural transition is essentially isochromic, in agreement with previous observations with native tRNAs. The current results suggest that changes in local divalent ion concentration in the ribosome could profoundly affect the global conformations of tRNAs during the translation cycle.

A principal feature of the tertiary[1] structure of native yeast tRNA^{Phe} is its L-shaped conformation, defined by the approximately perpendicular arrangement of the anticodon and aminoacyl helix stems [refined structures in Holbrook et al. (1978) and Hingerty et al. (1978); see also Stout et al. (1976)]. Previous spectroscopic studies have demonstrated that the native tRNA (tertiary) structure is not formed in the absence of divalent cations, even at temperatures that are well below the principal hyperchromic transition and in high concentrations of monovalent ions (Ishida & Sueoka, 1968; Cohn et al., 1969; Römer et al., 1970; Danchin & Gueron, 1970; Eisinger et al., 1970; Beardsley et al., 1970; Robison & Zimmerman, 1971; Willick & Kay, 1971; Lynch & Schimmel, 1974a; Stein & Crothers, 1976; Labuda et al., 1977). Calorimetric studies have confirmed that the low-temperature structures of several tRNAs (absence *vs* presence of Mg^{2+} ions) are thermodynamically distinct, with the binding of Mg^{2+} and formation of native tertiary structure being accompanied by an increase in entropy (Rialdi et al., 1972; Lynch & Schimmel, 1974a; Privalov et al., 1975; Hinz et al., 1977; Privalov & Filimonov, 1978).

Although the existence of a divalent cation-dependent transition leading to the formation of native tRNA is well-established, the nature of the conformational transition is not known in detail, except that it is essentially isoenthalpic and isochromic (see Discussion). One approach to the characterization of this transition would involve a description of the relative (angular) positions of the acceptor and anticodon stems (comprising the termini of the "L") as a function of the concentration of Mg^{2+} ions, since the positions of these arms undoubtedly reflect the formation of tertiary interactions within the tRNA core (Holbrook et al., 1978; Hingerty et al., 1978; Stout et al., 1976; Moras et al., 1980; Romby et al., 1987). To examine this issue, we have determined the apparent interstem angle of yeast tRNA^{Phe} as a function of Mg^{2+} ion concentration throughout the tertiary folding transition, at temperatures that are well below the start of the main, hyperchromic (melting) transition.

Using an unmodifed yeast tRNA^{Phe} RNA molecule with elongated anticodon and acceptor stems (designated E-[tRNA^{Phe}]),[2] we and others (Friederich et al., 1995; Nakamura et al., 1995) have recently demonstrated that the angle subtending the acceptor and anticodon stems (for millimolar Mg^{2+} ion concentrations) is approximately equal to the corresponding value for the native (fully modified) tRNA in the crystal. For the solution study, Friederich et al. (1995) employed the method of transient electric birefringence (TEB) (Fredericq & Houssier, 1973; Hagerman, 1996; Hagerman & Amiri, 1996), a hydrodynamic method that is sensitive to the interstem angle of the extended tRNA by virtue of the consequent differences in rotational diffusion constants (Vacano & Hagerman, 1997). This method has also been used to define the conformational transitions

† This work was supported by a grant from the National Institutes of Health (GM 52557 to P.J.H.).

* Corresponding author: Paul J. Hagerman, Department of Biochemistry, Biophysics, and Genetics, B-121, University of Colorado Health Sciences Center, 4200 E. Ninth Ave., Denver, Colorado 80262. Phone: (303) 315-8305. Fax: (303) 315-5467. E-mail: paul.hagerman@uchsc.edu.

⊗ Abstract published in *Advance ACS Abstracts,* May 1, 1997.

[1] In the current work, tertiary structure refers to the higher-order arrangement of the (preformed) tRNA cloverleaf secondary structure.

[2] Abbreviations: TEB, transient electric birefringence; E[tRNA^{Phe}], extended tRNA^{Phe}; P_i, inorganic phosphate; bp, base pair.

S0006-2960(97)00066-4 CCC: $14.00

induced by Mg^{2+} in RNA bulges (Zacharias & Hagerman, 1995a,b) and in self-cleaving "hammerhead" RNAs (Gast et al., 1994; Amiri & Hagerman, 1994, 1996).

In the current work, the TEB approach has been used in conjunction with the extended tRNA constructs to examine the Mg^{2+}-induced transition; the principal finding is that the transition involves a major conformational rearrangement with a substantial (~70°) reduction in the interstem angle. The major transition is complete in sub-millimolar concentrations of Mg^{2+}, although a second, minor rearrangement takes place in the 1−5 mM range. The Mg^{2+}-induced transition apparently does not represent a significant (net) change in secondary structure; it is essentially isochromic, in conformance with earlier observations using native tRNAs. Moreover, the current experiments were performed at temperatures that are at least 20 °C below the onset of the thermal unfolding (hyperchromic) transition for the unmodified tRNA constructs.

MATERIALS AND METHODS

Plasmid Constructs. The construction, characterization, and purification of plasmids used in the production of the extended yeast $tRNA^{Phe}$ heteroduplex and linear control duplex have been described previously (Friederich et al., 1995). Briefly, double-stranded oligonucleotides corresponding in sequence to the 5′ half (dhU, D-loop) and the 3′ half (TψC, T-loop) of yeast $tRNA^{Phe}$ (plus short flanking sequences) were inserted into the *Hin*dIII cloning sites of the parent plasmids, pGJ122A and pGJ122B, respectively. These parent plasmids are derivatives of the plasmid pGEM7Zf+ (Promega) in which the DNA sequences between positions 2692 and 72 of pGEM7Zf+ have been replaced by a fragment containing a T7 promoter, a 136-base pair (bp) template with a central *Hin*dIII insertion site, and a downstream *Sma*I site. The resultant plasmids are designated pGJ122A or pGJ122B, depending on the orientation of the 136 bp template. The derivative plasmids, designated pGJ122A9 and pGJ122B11, when transcribed and annealed, yield an E[$tRNA^{Phe}$] heteroduplex molecule in which the anticodon and acceptor stems have each been extended by approximately 70 bp. Plasmids containing the templates for the linear control have been designated pGJ122A38 and pGJ122B38. Annealing the RNA transcripts from these latter two plasmids results in a fully duplex linear control RNA molecule (174 bp).

Transcription, Purification, and Production of Double-Stranded (ds) RNA. Plasmid constructs to be used for transcription reactions were digested with *Sma*I (New England Biolabs, NEB) overnight at room temperature. After the digest was complete, the plasmids were incubated with proteinase K (0.5 mg/mL) and SDS (1%) at 42 °C for 30 min, followed by extraction with phenol/chloroform and precipitation with ethanol. Transcription reactions were performed as described previously (Amiri & Hagerman, 1994; Zacharias & Hagerman, 1995a,b; Friederich et al., 1995). A standard T7 transcription reaction mixture consisted of 0.06−0.18 μg/mL *Sma*I-digested plasmid DNA, T7 RNA polymerase, and transcription buffer: 40 mM Tris-HCl (pH 8.1), 0.1 mM spermidine, 5 mM DTT, 0.001% Triton, each NTP (2.5 mM), and 20 mM $MgCl_2$. After 2 h at 37 °C, the reaction mixture was terminated by the addition of NaEDTA at pH 8.0 (50 mM final), followed by extraction with phenol/chloroform and precipitation with 2-propanol. A 1 mL transcription reaction mixture typically yielded 0.5−1.0 mg of single-stranded RNA. T7 RNA polymerase was prepared as described previously (Shen & Hagerman, 1994). Single-stranded RNAs were examined for any degradation on denaturing (8 M urea) polyacrylamide gels (monomer/bis ratio of 19/1) with TBE running buffer [90 mM Tris-borate (pH 7.2) and 2.0 mM NaEDTA].

Transcripts were annealed in equimolar amounts to form either the E[$tRNA^{Phe}$] heteroduplex or the 174 bp linear duplex control. Annealing reactions (0.5 μg of total RNA/μL) were performed in 100 mM Tris-HCl (pH 6.5), 100 mM NaCl, 5 mM NaEGTA, and 10 mM NaEDTA (pH 8.0). Samples were heated to 95 °C for 5 min followed by cooling to room temperature over a period of 30 min. The double-stranded RNA molecules were purified further by running the complete annealing reaction on 6% polyacrylamide gels (monomer/bis ratio of 29/1, TBE running buffer). The band of interest was visualized by brief UV shadowing and was excised from the gel, macerated, and suspended overnight at 4 °C in 0.5 M NaOAc, 50 mM Tris-HCl, and 10 mM NaEDTA (pH 8.1). After elution, the double-stranded RNAs were precipitated with 2-propanol and stored at −20 °C in 200 mM NaCl, 50 mM Tris-HCl (pH 8.1), and 10 mM NaEDTA (pH 8.0).

Lead (Pb^{2+}) Cleavage Reactions. The stored duplex and heteroduplex RNAs were precipitated and resuspended in 30 mM Tris-HCl (pH 8.1). Pb^{2+} cleavage reactions were performed following the protocol of Pan et al. (1991) with some modifications. The E[$tRNA^{Phe}$] construct (2 μM) was incubated for 30 min in 15 mM (morpholino)propanesulfonic acid (MOPS, pH 7.0) containing 0, 1, 5, or 15 mM $MgCl_2$ and 0.4 mM lead acetate at either 37 or 50 °C for 30 min. The Pb^{2+} cleavage reaction was also carried out in 15 mM MOPS (pH 7.5) and 5 mM $MgCl_2$. In addition, in one set of experiments, the lead acetate was added before the addition of the buffer containing the $MgCl_2$. After the completion of the cleavage reaction, NaEDTA (pH 8.0) was added to a final concentration of 25 mM; the cleaved RNAs were then precipitated in order to remove the lead acetate. The precipitated RNA was resuspended in 30 mM Tris-HCl (pH 8.0), 15 mM $MgCl_2$, and T4 polynucleotide kinase (NEB) and incubated at 37 °C for 45 min. After the addition of 30 mM Tris-HCl (pH 7.5), 8 mM DTT, [γ-^{32}P]ATP, and T4 polynucleotide kinase, the reaction mixture was incubated at 37 °C for another 30 min. After the incubation was complete, NaEDTA (pH 8.0) was added to a final concentration of 25 mM; the RNA was then precipitated with ethanol and held for 1 h at −20 °C. The precipitated RNA was resuspended in 30 μL of diethyl pyrocarbonate (DEPC)-treated water, and one-third of the reaction mixture was used for gel analysis.

The E[$tRNA^{Phe}$] species was also end-labeled by incubating 2 μM RNA with calf intestinal phosphatase (CIP) for 30 min at 37 °C, extracted once with phenol/chloroform, and ethanol precipitated for 1 h at −20 °C. The precipitated RNA was incubated with T4 polynucleotide kinase (NEB) in 70 mM Tris-HCl (pH 7.6), 10 mM $MgCl_2$, 5 mM DTT, and [γ-^{32}P]ATP for 30 min at 37 °C, extracted with phenol/chloroform, and ethanol precipitated for 1 h at −20 °C. The precipitated RNA was resuspended in 30 μL of DEPC-treated water, and one-third of the reaction mixture was used for gel analysis. The Pb^{2+}-treated and end-labeled E[$tRNA^{Phe}$]

constructs were analyzed on denaturing 8 M urea, 8% polyacrylamide gels (monomer/bis ratio of 19/1) with TBE running buffer; gels were run at 40−50 °C.

Buffered Free Magnesium Ion Concentrations. Reported magnesium ion concentrations are EDTA-buffered, free ion concentrations that have been estimated from the quadratic relation

$$M^2 + (E_T - M_T + 1/K_{app})M - M_T/K_{app} = 0$$

a rearrangement of the expression given by O'Sullivan (1969). In the above relation, M_T and E_T are the total (added) $MgCl_2$ and NaEDTA concentrations, respectively, M is the effective free Mg^{2+} ion concentration, and K_{app} is the apparent stability constant for MgEDTA (2.5×10^5 M^{-1}, pH 7) (O'Sullivan, 1969). For the purpose of ion buffering, the NaEDTA concentration has been held at 1.0 mM.

There are two principal sources of uncertainty in the effective free ion concentration. First, K_{app} increases with increasing pH; thus, K_{app} may be increased by as much as 2-fold at pH 7.2, where most of the measurements are performed. This shift would result in a lowering of the free ion concentration, and a leftward shift in the transition depicted in Figure 3 by as much as 0.3 log at the lowest $MgCl_2$ concentrations. Second, the free Mg^{2+} concentrations may be further reduced through ion binding to RNA. The molar concentrations of RNA molecules used in the TEB experiments range from 1 to 3 μM. Since the tRNA core possesses several strong binding sites for Mg^{2+}, the effective concentration of those sites could range from 5 to 15 μM. Although we have made no attempt to refine this estimate, mass binding of Mg^{2+} ions by the tRNA would also shift the transition (Figure 3) to the left. Consequently, since our principal interest is the nature of the structural transition, we have made no effort to extract effective Mg^{2+} binding constants from the titration curves.

Gel Electrophoresis. Electrophoretic mobility assays were performed on 6% nondenaturing polyacrylamide gels (monomer/bis ratio of 29/1) at room temperature using increasing concentrations of Na^+ [10, 20, and 50 mM sodium phosphate (NaP_i) (pH 7.2) and 0.125 mM NaEDTA] with buffer recirculation. Three independent measurements were made at each Na^+ concentration. In addition, electrophoretic mobility assays were performed using 10 mM NaP_i (pH 7.2) in the presence of 5 mM $MgCl_2$. Relative electrophoretic mobility (μ_{rel}) refers to the ratio of the mobility of the E[$tRNA^{Phe}$] heteroduplex to that of a 174 bp linear duplex RNA.

Thermal Denaturation Analysis of the E[$tRNA^{Phe}$] Heteroduplex. The E[$tRNA^{Phe}$] heteroduplex was passed through a Sephadex (Pharmacia Biotech) G25 column (1/50 RNA sample/bed volume) equilibrated with 5 mM NaP_i (pH 7.2), 1 mM NaEDTA (pH 8.0), and 940 μM $MgCl_2$ (NaEDTA-buffered free Mg^{2+} concentration, 37 μM). Melting curve analysis was performed using a Varian Cary-1 spectrophotometer interfaced to a Dell XPS P133c computer. The concentration of RNA used for this analysis was 10 μg/mL. The temperature was increased at a rate of 3 °C per minute, from 2 to 70 °C with approximately one absorbance (A_{260}) acquired every 0.01 °C.

Hypochromicity Analysis. The E[$tRNA^{Phe}$] heteroduplex and 174 bp linear duplex RNA were passed through a Sephadex G25 column (1/50 RNA sample/bed volume) equilibrated with 5 mM NaP_i (pH 7.2), 1 mM NaEDTA, and 850 μM $MgCl_2$ (NaEDTA-buffered free Mg^{2+} concentration, 23 μM). Approximately 10 μg of each construct was diluted in NaP_i buffer to a volume of 0.95 mL; the absorbance at 260 nm (A_{260}) was measured using a Varian Cary 219 spectrophotometer at 20 °C. After the establishment of the baseline absorbance, the A_{260} was re-examined as the $MgCl_2$ concentration was increased in increments to yield free Mg^{2+} concentrations of up to 880 μM. After the addition of $MgCl_2$, the sample was pipetted two times, and the A_{260} was taken immediately and then again after 5 min. The observed A_{260} at a particular EDTA-buffered Mg^{2+} concentration was corrected for dilution on the basis of the volume of 20 mM $MgCl_2$ stock added.

Transient Electric Birefringence Measurements. Transient electric birefringence (TEB) measurements (Hagerman, 1996) were performed in essentially the same manner as described previously [*e.g.*, Amiri and Hagerman (1994, 1996), Zacharias and Hagerman (1995a,b), and Friederich et al. (1995)], except for the use of a smaller cell volume (35 μL). The temperature was maintained at 3.5 °C. The standard amplitude of the orienting electric field pulse was 1.5 kV (electrode spacing, 1.5 mm; 10 kV/cm). Measurements performed at lower field strengths revealed no differences in decay times or amplitudes. The duration of the pulse was 1.0 μs, with a repetition frequency of 1 Hz. The decay curves were accumulated and averaged on a LeCroy 9310 digitizing/averaging oscilloscope and were stored as files on floppy disks. From 128 to 1000 individual decay curves were accumulated per average. Identical averages were accumulated for buffer alone in order to correct for water birefringence. The data files were transferred to 80486-based (Dell) computers, where the decay profiles were analyzed using software written in the laboratory. The analysis of the decay curves is based on the Levenberg−Marquardt (LM) method (Press et al., 1992).

The RNA molecules used for TEB analysis were reprecipitated from the storage buffer and resuspended in TEB buffer [5 mM NaP_i (pH 7.2) and 1 mM NaEDTA] with the addition of 0−7 mM $MgCl_2$. The RNA species were passed through a Sephadex G25 column (1/50 RNA sample/bed volume) equilibrated with the appropriate TEB buffer plus $MgCl_2$. TEB measurements were also performed with increasing NaP_i concentrations (10, 15, and 20 mM) in the absence of Mg^{2+} ions. In addition, TEB measurements were performed in 15 mM NaP_i (pH 7.2) with increasing free Mg^{2+} ion concentrations (4−265 μM). TEB cell resistances were measured prior to each TEB measurement using an AC ohmmeter. The amount of RNA used for TEB measurements was 4.5−9 μg per 35 μL. After each series of measurements, the RNA was examined on nondenaturing polyacrylamide gels; no evidence of RNA degradation or strand separation was observed for any measurement.

Ratios of the terminal decay times (τ_{tRNA}/τ_{174}) were analyzed as described elsewhere [Friederich et al., 1995; see also Vacano and Hagerman (1997) and Zacharias and Hagerman (1997)]. The helix parameters used in this study were those of double-stranded RNA: persistence length, 700 Å; helix rise, 2.8 Å/bp; and hydrodynamic radius, 13 Å (Gast & Hagerman, 1991; Kebbekus et al., 1995). As discussed elsewhere (Zacharias & Hagerman, 1995a; Vacano & Hagerman, 1997), the derived angles are remarkably insensitive to changes in the above helix parameters.

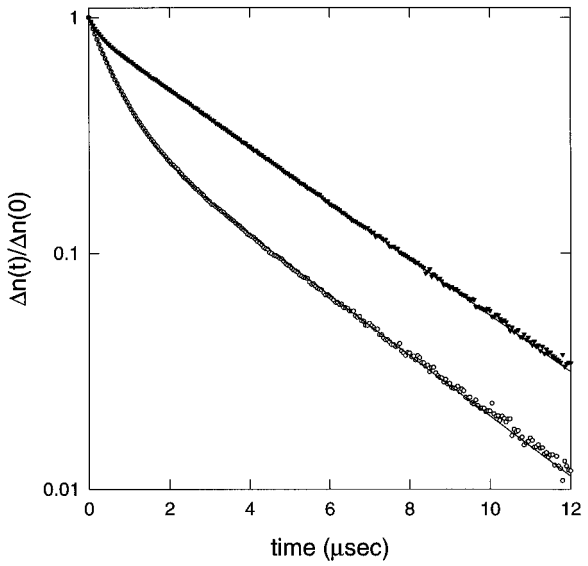

FIGURE 1: Representative birefringence decay curves of the E[tRNA^{Phe}] molecule (○) and the 174 bp dsRNA linear control molecule (▼) in the absence of Mg^{2+}. For each curve, the actual data points are displayed along with double-exponential fits to the data (solid lines). The experimental decay curves were fit using the Levenberg−Marquardt (LM) method (Press et al., 1992; see Materials and Methods).

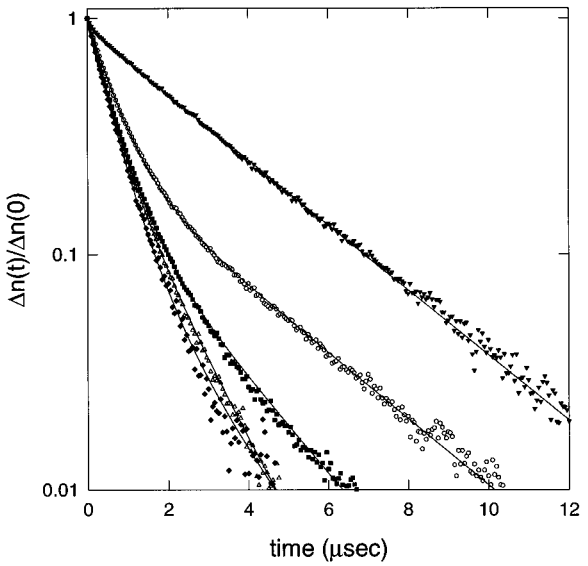

FIGURE 2: Representative birefringence decay curves of the E[tRNA^{Phe}] molecule in the presence of various concentrations of (buffered) free Mg^{2+} ions: 4 μM (○), 37 μM (■), 265 μM (△), and 6 mM (◆). Also shown are data for the 174 bp dsRNA linear control molecule (2 mM Mg^{2+}, ▼). For each curve, the actual data points are displayed along with double-exponential fits to the data (solid lines, see Materials and Methods).

RESULTS

The Angle between the Acceptor and Anticodon Stems of the tRNA^{Phe} Heteroduplex Is Substantially Reduced upon the Addition of Mg^{2+} Ions. It had been demonstrated previously (Friederich et al., 1995) that the relative electrophoretic mobility of the E[tRNA^{Phe}] construct is strongly dependent on Mg^{2+} ion concentrations in the sub-millimolar range, with mobilities decreasing dramatically (relative to a linear duplex RNA control) as the concentrations increased from zero to *ca.* 200 μM Mg^{2+}. Although the reduction in mobility is consistent with a reduction of the angle subtending the anticodon and acceptor stems (greater departure from colinearity) upon the addition of magnesium [*e.g.*, Cooper and Hagerman (1989), Gast et al. (1994), Bassi et al. (1995), Zacharias and Hagerman (1995a,b), and Leehey et al. (1995)], absolute values for the interstem angles are not readily obtainable from gel mobility data. Accordingly, we have used TEB to quantify the magnesium dependence of the interstem angle for the yeast tRNA^{Phe} construct. Representative decay curves for the heteroduplex and linear control RNAs are presented in Figures 1 and 2. The τ ratios (τ_{tRNA}/τ_{174}) for 26 sets of measurements are presented in Figure 3A. In Figure 3B, the τ ratios have been converted to apparent interstem angles as described elsewhere (Friederich et al., 1995; Zacharias & Hagerman, 1995a; Vacano & Hagerman, 1997) and are plotted as a function of Mg^{2+} ion concentration.

It is evident (Figure 3B) that, for free Mg^{2+} ion concentrations below 1−10 μM, the apparent interstem angles are quite large, equivalent to the two stems lying within ∼30° of colinearity. As the Mg^{2+} ion concentration increases from about 10 to 200 μM, there is a dramatic reduction in the apparent angle to approximately 70°. Further addition of Mg^{2+} results in slight broadening of the angle to a final value in the 80−90° range (Figure 3B; Friederich et al., 1995; M. W. Friederich and P. J. Hagerman, unpublished observations). For Mg^{2+} ion concentrations above 6−8 mM, a small amount (∼1−2%) of aggregation was detected as a slight flaring of the end of the terminal decay component. However, the relative mobility of the tRNA construct reached

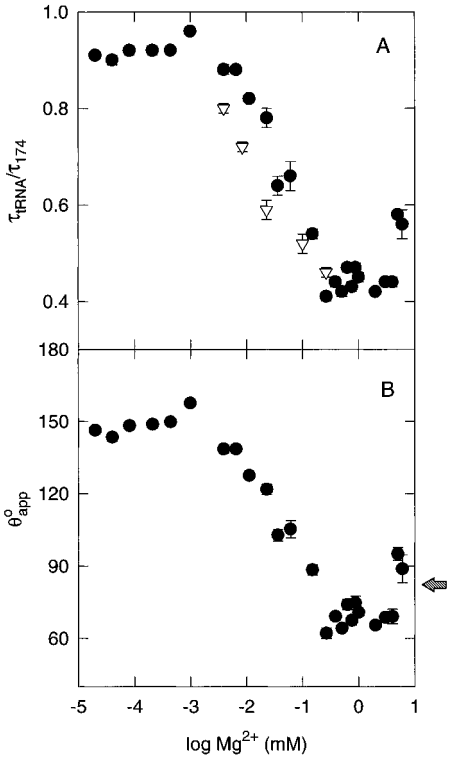

FIGURE 3: (A) Plot of the ratio, τ_{tRNA}/τ_{174}, as a function of free Mg^{2+} concentration in the presence of either 5 mM NaP_i (●) or 15 mM NaP_i (▽). (B) Plot of the apparent (*i.e.*, average) interstem angle of the E[tRNA^{Phe}] heteroduplex as a function of the free Mg^{2+} concentration. For reference, τ_{174} varies from 3.60 to 3.15 μs as the Mg^{2+} concentration is increased from zero to 6.0 mM. Note that, below *ca.* 10 μM free Mg^{2+} ion, the reported concentrations are subject to substantial uncertainty (see Materials and Methods). The hatched arrow to the right of the graph corresponds to the interhelix angle reported for yeast tRNA^{Phe} from X-ray crystallography (Holbrook et al., 1978).

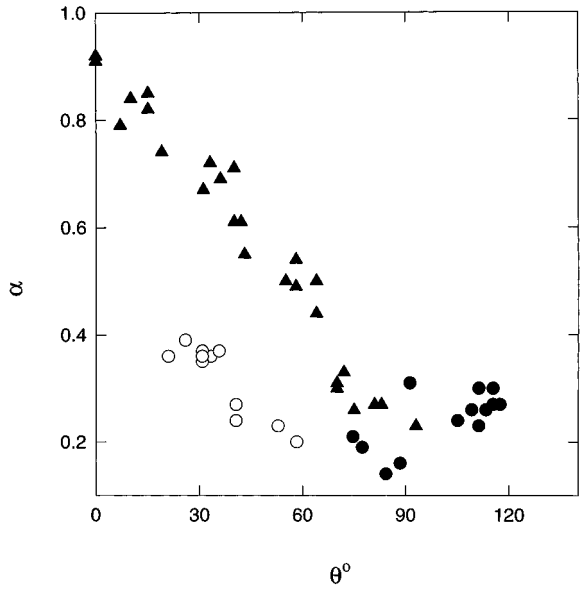

FIGURE 4: Plot of the fractional (slow) amplitude (α) of the birefringence decay profile as a function of the calculated bend angle of the E[tRNA^{Phe}] heteroduplex: (○) 0 to 23 μM Mg^{2+} and (●) 36 μM to 6 mM Mg^{2+}. For comparison, the relative amplitudes for a series of A_n and U_n bulges are displayed (▲, 2 mM Mg^{2+}) (Zacharias & Hagerman, 1996).

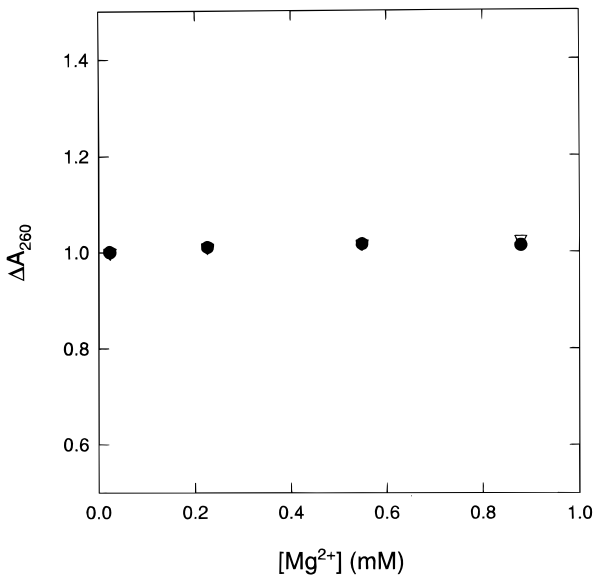

FIGURE 5: Plot of the change in A_{260} as a function of Mg^{2+} concentration for the E[tRNA^{Phe}] construct (▽) and for the 174 bp linear duplex RNA (●). The change in A_{260} is defined as the ratio of the absorbance (at 260 nm) at a particular Mg^{2+} concentration to the absorbance at 23 μM Mg^{2+}.

a constant value above ~4 mM, indicative of a limiting interstem angle.

It is important to bear in mind that the observed τ ratios reflect the population distribution of interstem angles at any given Mg^{2+} ion concentration, hence the "apparent" designation for the angles. For a nonhelix element in which there is broad angle dispersion (increased flexibility relative to the surrounding helix), the τ ratios represent an average over the ensemble, the nature of which will depend not only on the breadth of the angle distribution but also on whether the conformers are in fast or slow exchange on the time scale (microseconds) of the birefringence response (Shen & Hagerman, 1994; Zacharias & Hagerman, 1996, 1997; Vacano & Hagerman, 1997). For the yeast tRNA^{Phe} (transcript) core in the presence of at least 1 mM Mg^{2+} ions, recent experimental evidence suggests that the 80−90° angle is well-defined, possessing little or no additional flexibility over that expected for pure RNA helix [Nakamura et al., 1995; analyzed in Hagerman (1997); M. W. Friederich et al., in preparation]. These experimental findings are supported by a recent normal mode analysis of Nakamura and Doi (1994); the lowest normal mode, corresponding to hinge flexure, was only about 5°, even though the authors' computed *B* factors exceeded those found for the yeast tRNA^{Phe} crystal structure.

With decreasing Mg^{2+} ion concentrations (increasing τ ratio) within the transition region, the relative amplitude of the slow phase in the birefringence decay profile (Figure 4) remains much smaller than expected for relatively fixed bends (Zacharias & Hagerman, 1995a); such amplitude behavior is indicative of increased conformational freedom (Shen & Hagerman, 1994) and is considered in more detail elsewhere (Vacano & Hagerman, 1997; Zacharias & Hagerman, 1997). Moreover, recent observations involving the torsional phasing of the tRNA core with a second bend center also indicate that the core becomes much more flexible as the angle distribution shifts to larger angles (M. W. Friederich et al., in preparation). Thus, the larger apparent angles (Figure 3) within and below the Mg^{2+} transition represent averages of broadened angle distributions; that is, the 150° "angle" is likely to reflect a relatively broad distribution of conformers. Nevertheless, the distribution means are clearly shifted to more open conformations.

The Mg^{2+}-Induced Reduction of the Acceptor−Anticodon Interstem Angle Is Not Associated with Any Significant Change in the Absorbance of the tRNA Heteroduplex. Although the thermal stability of an unmodified yeast tRNA^{Phe} transcript is slightly lower than its fully modified (native) counterpart, the onset of thermal unfolding for the transcript (>30 °C, ~80 mM K^+, no Mg^{2+}) (Sampson & Uhlenbeck, 1988) is still well above the temperature (3.5 °C) employed in the current investigation. We have confirmed that, under the conditions used in the current study, the absorbance of the tRNA heteroduplex changes by less than 1% below 25 °C (8.0 mM Na^+, 40 μM Mg^{2+}; data not shown). However, in order to determine whether there is any significant change in the UV absorbance of the tRNA construct upon the addition of Mg^{2+} at temperatures below the onset of the thermally induced unfolding (hyperchromic) transition, the absorbances of solutions containing either the tRNA heteroduplex or the control duplex were determined before and after the addition of aliquots of $MgCl_2$ at 20 °C (Figure 5). It is evident that the pronounced reduction in the interstem angle is not accompanied by any substantial change in absorbance. This observation is consistent with earlier reports that Mg^{2+} ion-induced structural changes in native tRNAs are associated with only marginal changes (<5%) in absorbance (Danchin & Gueron, 1970; Robison & Zimmerman, 1971; Danchin, 1972; Lynch & Schimmel, 1974a; Römer & Hach, 1975); such observations suggest that there is no *net* change in stacking interactions for the tRNAs.

Na^+ Ions Do Not Induce a Transition in the Interstem Angle of the tRNA Heteroduplex Comparable to the Transition Observed in the Presence of Mg^{2+} Ions. Despite a large body of evidence in support of a specific role of Mg^{2+} ions (and perhaps other divalent metal cations) in the formation of the native *tertiary* structure of tRNAs (see Discussion),

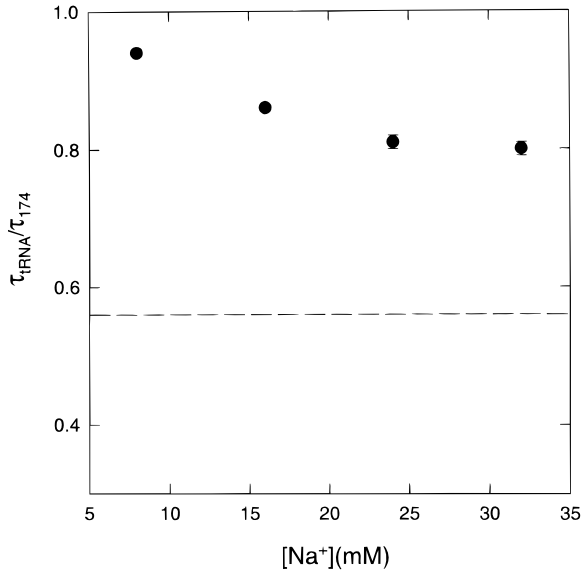

FIGURE 6: Plot of the ratio, τ_{tRNA}/τ_{174}, as a function of the Na^+ concentration in the absence of Mg^{2+} (●). The dashed line refers to the limiting ratio in the presence of 6 mM Mg^{2+} (8 mM Na^+).

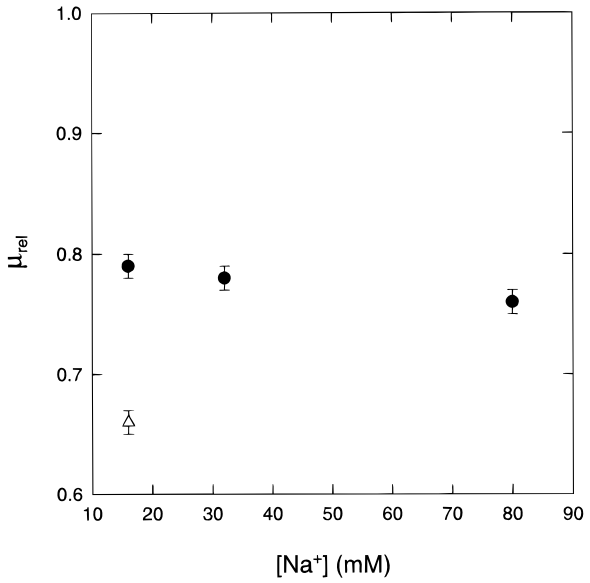

FIGURE 7: Plot of the relative electrophoretic mobilities, μ_{rel}, of E[$tRNA^{Phe}$] as a function of the Na^+ concentration. Mobility assays were performed on 6% nondenaturing polyacrylamide gels (29/1 monomer/bis ratio) at room temperature using increasing Na^+ concentrations: 16, 32, and 80 mM Na^+; 0.125 mM NaEDTA (●) with buffer recirculation. In addition, electrophoresis mobility assays were performed for 16 mM Na^+ in the presence of 5 mM Mg^{2+} (△). Relative electrophoretic mobility (μ_{rel}) refers to the migration distance of the E[$tRNA^{Phe}$] heteroduplex relative to that of a 174 bp linear duplex RNA. The data points are the average of three independent measurements (±1 SEM).

several reports have appeared in which the tertiary structures of tRNAs are presumed to be native in the presence of Na^+ ion concentrations exceeding ~30 mM and at temperatures below 20 °C (Römer & Hach, 1975; Yang & Crothers, 1972; Tropp & Redfield, 1983). Using the interstem angle as a sensitive indicator of tertiary structure, the above issue has been re-examined by performing a series of τ ratio measurements for several Na^+ ion concentrations in the absence of magnesium (Figure 6). From the τ ratio data, it is evident that, for monovalent ion concentrations of up to ~30 mM, the tRNA core does not assume a folded (L shape) conformation comparable to the one formed in the presence of Mg^{2+}. These TEB results are reinforced by the observation that the relative mobilities (μ_{rel}) of the tRNA construct are much higher (larger interstem angle) in Na^+ buffers than in Mg^{2+} (or Mg^{2+}/Na^+) buffers (Figure 7). Thus, for Na^+ ion concentrations of up to 80 mM, there is no evidence of a significant trend toward the smaller interstem angles induced by magnesium at Mg^{2+} ion concentrations nearly 2 orders of magnitude lower.

Low Na^+ ion concentrations appear to have a small, synergistic effect on the Mg^{2+} ion-induced transition (Figure 3A). This latter effect may reflect a small screening contribution from the monovalent ions and would be distinct from the well-described competition between Na^+ and Mg^{2+} ions observed at higher Na^+ ion concentrations (see Discussion). However, the effect of Na^+ ions presented in Figure 3A has not been examined in a systematic fashion and may also reflect contributions of the Na^+ ions to the strength of the Mg^{2+}−EDTA interaction.

The Extended $tRNA^{Phe}$ Heteroduplex Undergoes Site-Specific, Lead-Induced Cleavage of the DihydroU Loop, Indicative of the Native DihydroU−TψC Loop Juxtaposition. Lead ions induce the specific cleavage of the dihydroU (D) loop of native yeast $tRNA^{Phe}$, with cleavage (primarily between residues U17 and G18) being dependent on the tertiary interaction between the D and TψC loops (Werner et al., 1976; Sampson et al., 1987; Kryzyzosiak et al., 1988; Behlen et al., 1990). Moreover, the specificity of cleavage is essentially unchanged in the unmodified yeast $tRNA^{Phe}$ transcript (Sampson et al., 1987; Behlen et al., 1990). Thus, lead-induced cleavage represents a convenient assay of the proper coordination between the D and TψC loops in the E[$tRNA^{Phe}$] heteroduplex employed in the current study. Accordingly, the E[$tRNA^{Phe}$] heteroduplex was subjected to lead cleavage at various Mg^{2+} ion concentrations (0, 1, 5, and 10 mM) and temperatures (37 and 50 °C). Site-specific cleavage was observed in both 1 and 5 mM Mg^{2+} concentrations and at both 37 and 50 °C (Figure 8), consistent with earlier observations for both native and unmodified $tRNA^{Phe}$ species, and indicating correct coordination between the D and TψC loops in the E[$tRNA^{Phe}$] construct. Specific cleavage was reduced in solutions containing 15 mM Mg^{2+}, possibly due to competition between the binding of the two ions (Behlen et al., 1990); cleavage was also reduced in the absence of Mg^{2+} ions, presumably reflecting the loss of coordination between the two loops. This last observation is consistent with the TEB observations (Figure 3B) that indicate a more open, flexible tRNA core in the absence of Mg^{2+} ions, with the concomitant loss of interloop coordination.

DISCUSSION

In a previous investigation of the tertiary conformation of yeast $tRNA^{Phe}$, it was demonstrated using TEB that the angle between the anticodon and acceptor stems of the unmodified tRNA core (89 ± 4°) (Friederich et al., 1995) is quite similar to the corresponding value (~82°) in the crystal (Holbrook et al., 1978), both structures being studied in the presence of Mg^{2+} ions. In the current work, the TEB analysis of $tRNA^{Phe}$ has been extended by demonstrating that millimolar concentrations of divalent (Mg^{2+}) ions are required to form the final L-shaped conformation. In the absence of Mg^{2+}

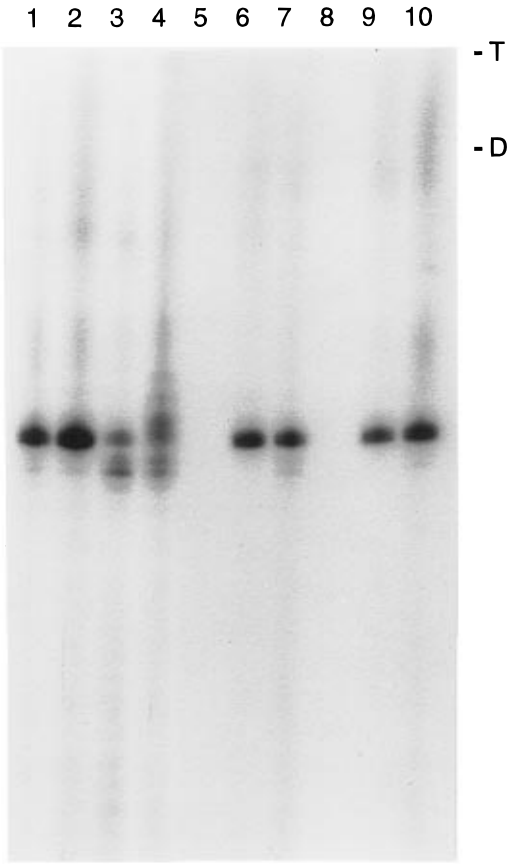

FIGURE 8: Lead acetate cleavage analysis of the E[tRNA^{Phe}]. The E[tRNA^{Phe}] molecule (2 μM) was first subjected to cleavage by lead acetate (400 μM) in 15 mM MOPS (pH 7.0 or 7.5) containing 0, 1, 5, or 15 mM $MgCl_2$ at 37 °C (data not shown) or 50 °C for 30 min. The specific cleavage site was labeled by incubating the cleaved molecules with T4 polynucleotide kinase and [γ-^{32}P]ATP. The E[tRNA^{Phe}] was also end-labeled in order to size the uncleaved full-length ssRNA transcripts by incubating 2 μM molecule with CIP followed by end labeling with T4 polynucleotide kinase and [γ-^{32}P]ATP. The reactions were analyzed on a denaturing 8% polyacrylamide gel containing 8 M urea and 20% formamide. Lanes: (1) 1 mM $MgCl_2$, 50 °C; (2) 5 mM $MgCl_2$, 50 °C; (3) 15 mM $MgCl_2$, 50 °C; (4) no $MgCl_2$, 50 °C; (5) blank; (6) 15 mM MOPS (pH 7.5) and 5 mM $MgCl_2$, 37 °C; (7) 15 mM MOPS (pH 7.5) and 5 mM $MgCl_2$, 50 °C; (8) blank; (9) lead acetate added before the addition of 5 mM $MgCl_2$, 37 °C; and (10) lead acetate added before the addition of 5 mM $MgCl_2$, 50 °C. Arrows to the right of the image are positions of full-length, single-stranded RNAs: (D) D-loop strand and (T) TψC-loop strand.

ions, the native structure is not achieved in Na^+ ion concentrations as high as 80 mM, nor is there any evidence of a trend toward the L-shaped form with increasing monovalent ion concentrations. The current observations thus provide a structural framework for the substantial body of earlier thermodynamic and spectroscopic work on yeast tRNA^{Phe} and other tRNA species from both prokaryotic and eukaryotic (cytoplasmic) sources.

Sub-Millimolar Concentrations of Mg^{2+} Ions Induce a Substantial Rearrangement of the Acceptor and Anticodon Stems of Yeast tRNA^{Phe}, Leading to the Native, L-Shaped Conformation. In the absence of Mg^{2+} ions, the *apparent* mean interstem angle is quite large (~150°). Although this apparent angle value reflects a degree of conformational flexibility (broad angle dispersion) that is much greater than that of the native form (Nakamura & Doi, 1994; Hagerman, 1997; M. W. Friederich et al., in preparation), the Mg^{2+}-free conformers are, on average, much more open than the native form; that is, the larger apparent angle is not a simple consequence of additional flexibility of the native conformation (Vacano & Hagerman, 1997; Zacharias & Hagerman, 1997). Upon addition of sub-millimolar concentrations of Mg^{2+} ions (2−200 μM), the tRNA core undergoes a dramatic conformational rearrangement that involves an ~80° reduction in the interstem angle. From 200 μM to 4 mM Mg^{2+}, there is a gradual, small increase in the interstem angle to a final value in the 80−90° range. The plateau above 4 mM is based on both TEB and gel measurements.

The current results are in accord with previous descriptions of a Mg^{2+}-induced conformational transition for various tRNAs. Römer et al. (1970) demonstrated a small, albeit significant increase in the sedimentation coefficient of yeast tRNA^{Phe} as the Mg^{2+} ion concentration was increased from 10 to 100 μM (~10 mM Na^+), with no further change in the *S* value above 100 μM Mg^{2+}. Similar behavior was observed using Y base fluorescence (Eisinger et al., 1970), molar ellipticity (Willick & Kay, 1971; Robison & Zimmerman, 1971), and electron paramagnetic resonance (EPR, Mn^{2+} ions) (Danchin & Gueron, 1970). In particular, Danchin and Gueron (1970) defined three zones of Mn^{2+} binding to tRNA on the basis of Scatchard plots: zone I, Mn^{2+}/phosphate < 0.05 (cooperative Mn^{2+} binding to "strong" sites); zone II, 0.05 < Mn^{2+}/P < 0.25 (remaining strong sites bound); and zone III, 0.25 < Mn^{2+}/P (further Mn^{2+} binding to weak sites). For the current work (Mg^{2+} ions, 400−800 μM RNA phosphate), zone I corresponds to [Mg^{2+}] < 40 μM, zone II to [Mg^{2+}] = 40−160 μM, and zone III to [Mg^{2+}] > 160 μM. Thus, the early EPR study defines regions that correspond approximately to the lower plateau, transition region, and upper plateau for the conformational transition observed in the current work. Similar conclusions were made by Robison and Zimmerman (1971) on the basis of both molar ellipticity and size-exclusion chromatography measurements in the presence of Mg^{2+} ions. In this regard, it should be noted that Mg^{2+}, Mn^{2+}, and Co^{2+} ions all display comparable binding affinities to strong sites on tRNAs (Danchin, 1972). Moreover, a variety of divalent cations (including Mg^{2+}, Mn^{2+}, Ca^{2+}, Sr^{2+}, and Ba^{2+}) appear to stabilize *Escherichia coli* tRNA^{Trp} in a form that is active in aminoacylation (Ishida & Sueoka, 1968).

Monovalent Cations Do Not Lead to the Formation of the Native, L-Shaped Conformation of Yeast tRNA^{Phe}. The current results demonstrate that the global conformation of the extended yeast tRNA^{Phe} heteroduplex does not approach the canonical L-shaped structure even at Na^+ ion concentrations that are 100-fold higher than the Mg^{2+} ion concentrations required to approach the native conformation. Again, these results provide a specific structural framework for a large body of biochemical and thermodynamic work that supports a specific role of divalent cations, *i.e.*, that ionic strength is not an appropriate parameter for gauging the formation of native tRNA structure. Although the importance of valence-specific stabilization of DNA has been known for more than 40 years [Thomas, 1954; see also Dove and Davidson (1962) and Krakauer (1971)], the importance of ion valence was underscored for tRNA with the demonstration not only that monovalent cations (e.g., Na^+, K^+, Rb^+, Cs^+, NH_4^+, and $Tris^+$) were unable to produce tRNAs that are active in charging assays, but also that the addition

of the monovalent cations to Mg^{2+}−tRNAs actually inhibited charging (Ishida & Sueoka, 1968).

Subsequent studies of yeast $tRNA^{Phe}$ by Robison and Zimmerman (1971) provided support for the findings of Ishida and Sueoka (1968), namely that monovalent cations inhibit the Mg^{2+}-induced (tertiary) structural transition and cannot replace the divalent cations in promoting the formation of the native tertiary structure, even for monovalent cation concentrations as high as 2.0 M. Robison and Zimmerman (1971) also demonstrated that in the absence of Na^+ ions (10 mM Tris), yeast $tRNA^{Phe}$ exhibits charging activity for Mg^{2+} ion concentrations as low as 50 μM. Furthermore, Lynch and Schimmel (1974b) noted that the cooperativity of Mg^{2+} binding decreased as the concentration of monovalent salt increased. The inhibitory effects of Na^+ ions, both on the formation of the final tertiary structure and on the cooperativity of the Mg^{2+}-induced changes, were also noted by Labuda et al. [1977; see also Beardsley et al. (1970)], who pointed out that the formation of final tertiary structure (monitored by Y base fluorescence) was never achieved in the absence of Mg^{2+} ions (again, for Na^+ ion concentrations of up to 2.0 M). Finally, the calorimetric investigations of Privalov and co-workers (Privalov et al., 1975; Hinz et al., 1977; Privalov & Filimonov, 1978) demonstrated that both the cooperativity and thermal stabilities of several tRNAs (in buffers containing 1 mM Mg^{2+} ion) were diminished upon the addition of 150 mM Na^+. Thus, both the current findings and the bulk of the previous literature suggest that divalent cations are uniquely capable of promoting the formation of the native tertiary (L-shaped) conformation of the tRNA and that monovalent cations generally oppose the final folding transition.

The Conformational Transition Induced by Mg^{2+} Ions Is Not Accompanied by a Detectable Absorbance Change. One remarkable characteristic of the conformational transition is that it is essentially isochromic. This property of the transition suggests (but does not prove) that there is no substantial change in either the number or the nature of the stacking interactions within the tRNA core. In this regard, it should be noted that the current measurements were performed nearly 20 °C below the onset of the thermally induced melting transition as defined by the hyperchromicity profile. The current results are in agreement with a number of investigations of the divalent cation-induced transition in yeast $tRNA^{Phe}$ (Robison & Zimmerman, 1971; Römer & Hach, 1975), in unfractionated *E. coli* tRNA (Danchin & Gueron, 1970; Danchin, 1972), and in *E. coli* $tRNA^{Ile}$ (Lynch & Schimmel, 1974a); all reported essentially no change in absorbance accompanying the Mg^{2+}-induced transition (<5% change). This characteristic of the transition thus appears to be relatively general. It is noteworthy that the absence of an absorbance change accompanying the addition of Mg^{2+} ions has been (erroneously) interpreted to mean the absence of a conformational transition, *i.e.*, that the Na^+ and Mg^{2+} conformations of tRNAs are the same.

The Mg^{2+} Ion-Induced Transition to the Native Conformation of Yeast $tRNA^{Phe}$ Is an Isoenthalpic, Entropy-Driven Process. One additional property of the tertiary structural transition promoted by Mg^{2+} ions helps to define the origin of the stability of the native, L-shaped structure, namely that the transition is entropically driven (Rialdi et al., 1972; Lynch & Schimmel, 1974a; Privalov et al., 1975; Hinz et al., 1977; Privalov & Filimonov, 1978). Rialdi et al. (1972) first noted that the binding of Mg^{2+} ions to yeast $tRNA^{Phe}$ was not associated with any significant change in enthalpy but was accompanied by a large gain of entropy. Rialdi et al. (1972) suggested that the entropy gain was due, in part, to the release of water of hydration of the Mg^{2+} ions upon the binding of the divalent cations to the tRNA. Their suggestion is in accord with earlier studies of the binding of Mg^{2+} ions to nucleoside phosphates (Belaich & Sari, 1969) and to homoribopolymers (Krakauer, 1971); in both instances, the binding is entropy-driven and may reflect changes in the hydration state of the Mg^{2+} ions (Robinson & Stokes, 1959). Privalov et al. (1975) reinforced the earlier conclusion that the transition is entropy-driven and demonstrated that the overall transition enthalpy for tRNA unfolding is essentially independent of Mg^{2+} ion concentration. Privalov and Filimonov (1978) demonstrated that the fundamental character of the Mg^{2+} transition (isoenthalpic, positive entropy change) is quite general among tRNAs from *both E. coli* and yeast. The T_m's of the overall thermal unfolding transitions demonstrated considerable variation as a function of Mg^{2+} and/or Na^+ ion concentration; however, the transitions were always much more cooperative in the presence of Mg^{2+} ions than in their absence. Thus, the calorimetric investigations indicate that the Na^+− and Mg^{2+}−tRNAs are thermodynamically distinct structures.

On the basis of NMR measurements (longitudinal relaxation) of water molecules associated with Mn^{2+} ions, Cohn et al. (1969) suggested that Mn^{2+} binding to tRNA possessed both cooperative and site-specific character, possibly involving the coordination of a single divalent cation with several phosphates. Furthermore, those authors proposed that such coordination events brought secondary structural elements together to form a final tertiary structure. Lynch and Schimmel (1974a) analyzed the binding of Mg^{2+} ions to tRNA; they obtained a Hill cooperativity parameter of 2−3, with binding constants that were essentially independent of temperature (up to 30 °C, the highest temperature employed in the study). This latter observation is consistent with the isoenthalpic character of the Mg^{2+}-induced transition.

The cooperative ("strong") binding of two or three divalent cations may well correspond to one or more of the site-bound Mg^{2+} ions identified in the crystal of yeast $tRNA^{Phe}$ (Jack et al., 1976; Holbrook et al., 1977, 1978; Hingerty et al., 1978). Two likely candidates are the Mg^{2+} ion coordinating the D-loop residues G19 and G20 with the T-loop residues U59 and C60 and the Mg^{2+} ion coordinating phosphates in the tight (bp 8−12) turn between the 5′ strand of the acceptor stem and the 5′ strand of the D-loop stem; however, a direct mechanistic linkage between those ions and the conformational transition has not been established.

A Provisional Model for the Formation of the Final Tertiary Structure of Yeast $tRNA^{Phe}$. A dramatic change in the global conformation of the tRNA core is induced by Mg^{2+} ions in a manner that is ion-valence-specific (current and previous observations). This central observation, coupled with the fact that the Mg^{2+}-induced transition is isoenthalpic and entropy-driven (previous observations) and is isochromic (current and previous observations), allows one to draw several specific conclusions regarding the stabilization of the native tRNA structure. (i) The specific, tertiary hydrogen bonds identified in the crystal of yeast $tRNA^{Phe}$, while important for structural specificity, probably do not provide substantial *net* stabilization of the final structure. However,

by analogy to protein folding, the failure to form hydrogen bonds equivalent to those with water that are lost upon folding would lead to a net destabilization of the native structure. (ii) The final, tertiary folding transition is unlikely to be accompanied by a significant net change in the number or strength of stacking interactions. (iii) The formation of a relatively fixed native conformation is necessarily accompanied by a loss of (RNA) configurational entropy; the net positive entropy change must therefore be derived from other events, including partial loss of Mg^{2+} ion hydration, release of water bound via hydrogen bonds to bases and 2′-OH residues, and a net reduction in the thermodynamic association of monovalent counterions.

The significance of the above features is that they are likely to be of general importance in the tertiary folding of RNA. For yeast $tRNA^{Phe}$, failure to properly coordinate the closely apposed phosphates in the 8−12 turn, coupled with the failure to coordinate D and T loops via one or more interdigitated Mg^{2+} ions, would likely result in an opening of the core, with a corresponding increase in the interstem angle and a concomitant increase in angle dispersion. A similar set of observations has been made for the angles subtending helices I and II of the self-cleaving hammerhead RNA, where the addition of Mg^{2+} ions results in an ∼70° increase in the interstem angle for the extended hammerhead (Gast et al., 1994; Amiri & Hagerman, 1994).

POTENTIAL LIMITATIONS OF THE CURRENT STUDY

The Extended tRNA Constructs Employed in the Current Study Lack the Post-Transcriptional Modifications Present in the Native tRNA. The results of both the current investigation and previous TEB (Friederich et al., 1995) and EM (Nakamura et al., 1995) studies indicate that the anticodon−acceptor interstem angle of the unmodified (extended) tRNA heteroduplex is nearly identical to that of the native tRNA in the crystal (Holbrook et al., 1978). This concordance suggests that, whereas most transcriptional modification of the tRNA core may affect stability, such modifications do not result in any significant alteration of the tertiary structure of the tRNA core (at least for yeast $tRNA^{Phe}$). The close agreement between the solution and crystal-derived angles could be fortuitous, confounded by crystal packing forces and/or the helix extensions (see below); however, none of the base modifications in the $tRNA^{Phe}$ core appears to be essential for maintaining the integrity of its tertiary structure, and none is directly involved with any evident secondary or tertiary interactions (Holbrook et al., 1978). Moreover, the aminoacylation activity of the unmodified yeast $tRNA^{Phe}$ transcript is nearly equal to that of its native (fully modified) counterpart under appropriate ionic conditions (Sampson & Uhlenbeck, 1988; Dabrowski et al., 1995). This latter point argues that the global conformations (*i.e.*, the interstem angles) of the modified and unmodified species are not substantially different *in solution*, since the yeast $tRNA^{Phe}$ aminoacyl synthetase−$tRNA^{Phe}$ interaction requires both anticodon and acceptor stem contacts. Finally, Dabrowski et al. (1995) demonstrated that polypeptide synthesis with the unmodified transcript was nearly as effective (73−98%) as that with the native tRNA.

The Current tRNA Construct Possesses Extended Anticodon and Acceptor Stems. As noted above, Friederich et al. (1995) demonstrated that the interstem angle for E-[$tRNA^{Phe}$] is essentially identical to the corresponding angle for the native tRNA. Moreover, the current work has demonstrated that the extended construct retains the ability to undergo site-specific Pb^{2+} cleavage of the D loop, indicative of the specific juxtaposition of the D and T loops. In this regard, Swerdlow and Guthrie (1984) observed similar patterns of cleavage/protection for mature yeast $tRNA^{Phe}$ and a precursor that possesses an intervening sequence (IVS) at the end of the anticodon stem; the presence of the IVS radically alters the context of the anticodon triplet (and loop), moving the triplet into a section of an elongated stem. Thus, substantial alterations of local structure (including elongation of the anticodon stem) appear to have only modest effects on the tertiary structure of the tRNA core.

Finally, for their analysis of the global conformation of a self-cleaving hammerhead RNA, Amiri and Hagerman (1996) used helix extensions that were identical to those employed in the current investigation; they observed that the interstem angles were (i) fully active in self-cleavage (*i.e.*, the helix extensions displayed no inhibitory effects) and (ii) ion-valence-specific (*i.e.*, not ionic strength-dependent). These results are not surprising, since electrostatic interactions between the extended stems are expected to have only a minimal influence (if any) on the interstem angle for the angles and ionic conditions examined in the current work (Olmsted & Hagerman, 1994). Moreover, in support of this last statement, it is observed that, as the Mg^{2+} ion concentration is reduced from 5 to 0.2 mM, the interstem angle actually decreases slightly, a result that is opposite of expectation if bulk screening effects are dictating the arrangement of the two extended stems.

Further Consideration of the Analytical Approach. The combined experimental and computational methods comprising the TEB method have now been employed in several dozen studies of nonhelix elements in RNA (Hagerman, 1996). Where other methods are capable of providing similar information regarding conformation, the TEB results are generally in close agreement with the other studies (Hagerman & Amiri, 1996). Finally, the τ-ratio approach employed in the current investigation has been extensively discussed and analyzed and has been found to be quite robust as a method for extracting apparent angles. In the current work, the angles at the upper end of the Mg^{2+} transition are relatively well-defined (M. W. Friederich et al., in preparation); however, the apparent angles for the lower end of the transition, as in the transition region itself, probably represent population averages of broadly distributed angles rather than a single, well-defined angle.

CONCLUSIONS

Upon exposure to sub-millimolar concentrations of Mg^{2+} ions, the yeast $tRNA^{Phe}$ core undergoes a substantial conformational transition to a final, L-shaped tertiary structure. Although the transition involves a major change in the architecture of the tRNA core, the transition itself is isochromic, suggesting that there is no *net* change in the number or nature of stacking interactions. An important feature of this transition is that it is not principally governed by ionic strength effects; in particular, monovalent ions (*e.g.*, Na^{+}) are incapable of effecting the final (tertiary) folding transition. The current observations, coupled with the vast

previous literature which establishes the transition as essentially isoenthalpic (entropy-driven), suggest that the binding of a small set of Mg^{2+} ions is principally responsible for the tertiary transition.

The tRNA model remains a paradigm for the study of the formation of tertiary structure in RNA; the current work has underscored the potential of TEB to examine specific aspects of the tertiary structural transition. However, this investigation has also provided a direct demonstration of the potential for coupling the addition or removal of Mg^{2+} ions to major conformational transitions in tRNA during translation (Stein & Crothers, 1976; Yarus & Smith, 1995). In fact, this Mg^{2+} ion response may turn out to be a defining physical characteristic of certain classes of tRNAs [*e.g.*, Leehey et al. (1995)].

ACKNOWLEDGMENT

The authors thank Elsi Vacano for her help with the hydrodynamic analysis.

REFERENCES

Amiri, K. M. A., & Hagerman, P. J. (1994) *Biochemistry 33*, 13172−13177.
Amiri, K. M. A., & Hagerman, P. J. (1996) *J. Mol. Biol. 261*, 125−134.
Bassi, G. S., Møllegaard, N.-E., Murchie, A. I. H., von Kitzing, E., & Lilley, D. M. J. (1995) *Struct. Biol. 2*, 45−55.
Beardsley, K., Tao, T., & Cantor, C. R. (1970) *Biochemistry 9*, 3524−3532.
Behlen, L. S., Sampson, J. R., DiRenzo, A. B., & Uhlenbeck, O. C. (1990) *Biochemistry 29*, 2515−2523.
Belaich, J. P., & Sari, J. C. (1969) *Proc. Natl. Acad. Sci. U.S.A. 64*, 763−770.
Cohn, M., Danchin, A., & Grunberg-Manago, M. (1969) *J. Mol. Biol. 39*, 199−217.
Cooper, J., & Hagerman, P. J. (1989) *Proc. Natl. Acad. Sci. U.S.A. 86*, 7336−7340.
Dabrowski, M., Spahn, C. M. T., & Nierhaus, K. H. (1995) *EMBO J. 14*, 4872−4882.
Danchin, A. (1972) *Biopolymers 11*, 1317−1333.
Danchin, A., & Gueron, M. (1970) *Eur. J. Biochem. 16*, 532−536.
Dove, W. F., & Davidson, N. (1962) *J. Mol. Biol. 5*, 467−478.
Eisinger, J., Feuer, B., & Yamane, T. (1970) *Proc. Natl. Acad. Sci. U.S.A. 65*, 638−644.
Fredericq, E., & Houssier, C. (1973) *Electric Dichroism and Electric Birefringence*, Clarendon, Oxford, UK.
Friederich, M. W., Gast, F.-U., Vacano, E., & Hagerman, P. J. (1995) *Proc. Natl. Acad. Sci. U.S.A. 92*, 4803−4807.
Gast, F.-U., & Hagerman, P. J. (1991) *Biochemistry 30*, 4268−4277.
Gast, F.-U., Amiri, K. M. A., & Hagerman, P. J. (1994) *Biochemistry 33*, 1788−1796.
Hagerman, P. J. (1996) *Curr. Opin. Struct. Biol. 6*, 643−649.
Hagerman, P. J. (1997) *Annu. Rev. Biophys. Biomol. Struct.* (in press).
Hagerman, P. J., & Amiri, K. M. A. (1996) *Curr. Opin. Struct. Biol. 6*, 317−321.
Hingerty, B., Brown, R. S., & Jack, A. (1978) *J. Mol. Biol. 124*, 523−534.
Hinz, H.-J., Filimonov, V. V., & Privalov, P. L. (1977) *Eur. J. Biochem. 72*, 79−86.
Holbrook, S. R., Sussman, J. L., Warrant, R. W., Church, G. M., & Kim, S.-H. (1977) *Nucleic Acids Res. 4*, 2811−2820.
Holbrook, S. R., Sussman, J. L., Warrant, R. W., & Kim, S.-H. (1978) *J. Mol. Biol. 123*, 631−660.
Ishida, T., & Sueoka, N. (1968) *J. Biol. Chem. 243*, 5329−5336.
Jack, A., Ladner, J. E., & Klug, A. (1976) *J. Mol. Biol. 108*, 619−649.
Kebbekus, P., Draper, D. E., & Hagerman, P. (1995) *Biochemistry 34*, 4354−4357.
Krakauer, H. (1971) *Biopolymers 10*, 2459−2490.
Kryzyzosiak, W. J., Marciniec, M., Wiewiorowski, M., Romby, P., Ebel, J. P., & Giegé, R. (1988) *Biochemistry 27*, 5771−5777.
Labuda, D., Haertlé, T., & Augustyniak, J. (1977) *Eur. J. Biochem. 79*, 293−301.
Leehey, M. A., Squassoni, C. A., Friederich, M. W., Mills, J. B., & Hagerman, P. J. (1995) *Biochemistry 34*, 16235−16239.
Lynch, D. C., & Schimmel, P. R. (1974a) *Biochemistry 13*, 1841−1852.
Lynch, D. C., & Schimmel, P. R. (1974b) *Biochemistry 13*, 1853−1861.
Moras, D., Comarmond, M. B., Fischer, J., Weiss, R., Thierry, J. C., Ebel, J. P., & Giegé, R. (1980) *Nature 288*, 669−674.
Nakamura, S., & Doi, J. (1994) *Nucleic Acids Res. 22*, 514−521.
Nakamura, T. M., Wang, Y.-H., Zaug, A. J., Griffith, J. D., & Cech, T. R. (1995) *EMBO J. 14*, 4849−4859.
Olmsted, M., & Hagerman, P. J. (1994) *J. Mol. Biol. 243*, 919−929.
O'Sullivan, W. J. (1969) in *Data for Biochemical Research* (Dawson, R. M. C., Elliot, D. C., Elliot, W. H., & Jones, K. M., Eds.) pp 423−427, Oxford, University Press, London, UK.
Pan, T., Gutell, R. R., & Uhlenbeck, O. C. (1991) *Science 254*, 1361−1364.
Press, W. H., Vetterling, W. T., Teukolsky, S. A., & Flannery, B. P. (1992) *Numerical Recipes in Fortran: The Art of Scientific Computing*, pp 678−683, Cambridge University Press, Cambridge, UK.
Privalov, P. L., & Filimonov, V. V. (1978) *J. Mol. Biol. 122*, 447−464.
Privalov, P. L., Filimonov, V. V., Venkstern, T. V., & Bayev, A. A. (1975) *J. Mol. Biol. 97*, 279−288.
Rialdi, G., Levy, J., & Biltonen, R. (1972) *Biochemistry 11*, 2472−2479.
Robinson, R. A., & Stokes, R. H. (1959) *Electrolyte Solutions*, 2nd ed., pp 16−17, Butterworths, London.
Robison, B., & Zimmerman, T. P. (1971) *J. Biol. Chem. 246*, 110−117.
Romby, P., Moras, D., Dumas, P., Ebel, J. P., & Giegé, R. (1987) *J. Mol. Biol. 195*, 193−204.
Römer, R., & Hach, R. (1975) *Eur. J. Biochem. 55*, 271−284.
Römer, R., Riesner, D., & Maass, G. (1970) *FEBS Lett. 10*, 352−357.
Sampson, J. R., & Uhlenbeck, O. C. (1988) *Proc. Natl. Acad. Sci. U.S.A. 85*, 1033−1037.
Sampson, J. R., Sullivan, F. X., Behlen, L. S., DiRenzo, A. B., & Uhlenbeck, O. C. (1987) *Cold Spring Harbor Symp. Quant. Biol. 52*, 267−275.
Shen, Z., & Hagerman, P. J. (1994) *J. Mol. Biol. 241*, 415−430.
Stein, A., & Crothers, D. M. (1976) *Biochemistry 15*, 160−168.
Stout, C. D., Mizuno, H., Rubin, J., Brennana, T., Rao, S. T., & Sundaralingam, M. (1976) *Nucleic Acids Res. 3*, 1111−1123.
Swerdlow, H., & Guthrie, C. (1984) *J. Biol. Chem. 259*, 5197−5207.
Thomas, R. (1954) *Biochim. Biophys. Acta 14*, 231−240.
Tropp, J. S., & Redfield, A. G. (1983) *Nucleic Acids Res. 11*, 2121−2134.
Vacano, E., & Hagerman, P. J. (1997) *Biophys. J.* (in press).
Werner, C., Krebs, B., Keith, G., & Dirheimer, G. (1976) *Biochim. Biophys. Acta 432*, 161−175.
Willick, G. E., & Kay, C. M. (1971) *Biochemistry 10*, 2216−2222.
Yang, S. K., & Crothers, D. M. (1972) *Biochemistry 11*, 4375−4381.
Yarus, M., & Smith, D. (1995) in *tRNA: Structure, Function and Biosynthesis* (Söll, D., & RajBhandary, U. L., Eds.) pp 443−469, ASM Press, Washington, DC.
Zacharias, M., & Hagerman, P. J. (1995a) *J. Mol. Biol. 247*, 486−500.
Zacharias, M., & Hagerman, P. J. (1995b) *Proc. Natl. Acad. Sci. U.S.A. 92*, 6052−6056.
Zacharias, M., & Hagerman, P. J. (1996) *J. Mol. Biol. 257*, 276−289.
Zacharias, M., & Hagerman, P. J. (1997) *Biophys. J.* (in press).

BI970066F